Investigation on a micro-environment concept for MEA production process supported by numerical simulations

Ling Ma, Nadine Zimmerer, Jens Schäfer, Philipp Quarz, Thilo Heckmann, Philip Scharfer, Wilhelm Schabel, Jürgen Fleischer

The manufacturing process of membrane electrode assembly (MEA) generally takes place under climate control, as the base material used for membranes is well known for its hygroscopic properties. The large climate-controlled area for the whole assembly line does not only increase energy consumption, but also limits the further scalability of the production line. Within this article, a micro-environment concept for the MEA production based on a roll-to-roll (R2R) process was investigated. By using the Finite Element Method, a 3D numerical model has been established, in which the local climate control on different MEA production processes is covered. In particular, the influence of humidity on dimensional changes of the CCM, which in turn cause product deformation, is simulated. In addition, a gravimetric method was used to experimentally investigate the moisture absorption and release behavior of the MEA components under defined climatic conditions.

KEYWORDS: micro-environment, MEA production, water sorption, numerical simulation

1. INTRODUCTION

Along with the increasingly prominent environmental pollution and greenhouse effect problems, a transition to a decarbonized energy system is no longer evitable. In comparison to battery electrical vehicles (BEV), the fuel cell electric vehicles (FCEV) have shown a more promising decarbonization solution for trucks, buses, trains or similar, where a higher energy density is needed. The low-temperature polymer electrolyte membrane fuel cell (PEMFC) is often used in the automobile industry [Töpler & Lehmann, 2014]. The center piece of a PEMFC is the so called catalyst coated membrane (CCM), which consists of a polymer electrolyte membrane (PEM) with anode and cathode side catalyst layers (CLs). The PEM carries a couple of functionality decisive tasks, such as conducting the hydrogen protons and separating the fuel gas and the oxidant [Töpler & Lehmann, 2014]. Due to the combination of high electrochemical stability, high ion exchange capacity and proton conductivity and low gas permeability, the currently most commercially used membrane is produced by Chemours (former DuPont) with the tradename Nafion® [Jalani & Datta, 2005]. Nafion® is a branched polymer, consisting of a hydrophobic main group of polytetrafluoroethylene (PTFE) and side chains of perfluorinated vinyl ethers. The side groups end with hydrophilic ion exchange groups (SO_3^-). The complex structure of the Nafion® membrane is the subject of many studies from which various structural models have been developed ([Mauritz & Moore, 2004], [Kim et al., 2015], [Randová et al., 2015]). All of these models agree that the aggregation of the perfluorinated side chains results in the formation of ionic, hydrophilic clusters that are

embedded in a support structure of the hydrophobic main chains ([Goulet et al., 2015], [Kim et al., 2015]).

2. STATE OF THE ART

2.1. MEA MANUFACTURING

A PEMFC-stack is composed of two repeating units, namely the MEA and the bipolar plate. The MEA consists of a CCM, which is framed within the subgasket, for example by laminating two subgaskets onto each other with the CCM in between ([James et al., 2008], [Fey et al., 2010]). The subgaskets with active-area window in the middle can provide a mechanical enhancement for the CCM, a better endurance against the compression in the stacking process, as well as a precisely location control of the active area. Anode and cathode side gas diffusion layers (GDLs) are then put onto the subgasketed CCM, for example by gluing. As the thicknesses of membranes are only in the magnitude of microns, they are especially challenging for the overall handling process. Industrialized production commonly features several webs in a roll-to-roll process with different carrier films included.

A humidity change will cause water absorption in or release off the CCM and ultimately a dimensional change of the CCM will occur. Since the CCM is partially constrained on the edges by the subgaskets after the lamination process, the membrane swelling or shrinkage behavior is a critical factor for the assembly process. Hence, a clean room with temperature and humidity control is required for the MEA-fabrication, in order to avoid the humidity-induced stresses or deformations. As mentioned in the patent of Valentine et al., the ambient temperature and humidity level around 21 ± 2 °C and 42 ± 7 % are optimum for the MEA fabrication process [Valentine et al., 2009]. However, such an environmental control system involves both large capital investment and long-term energy consumption costs. The high investment reflects again in the final price of a fuel cell stack, which slows down the acceleration of commercialization of fuel cell technology. On top of that, the environmental control system is normally coupled with the plant building infrastructure, which needs to be taken into consideration in an early-stage planning phase and requires large retrofitting expenses for scaling-up.

2.2. HYGROSCOPIC BEHAVIOR OF THE MEA COMPONENTS

The dry Nafion® membrane is very hygroscopic [Töpler & Lehmann, 2014]. For this reason, within the MEA composite the membrane interacts preferable with water from the environment, so the investigation of this component is of great importance. During the sorption of water, the water interacts with the ionic clusters within the membrane structure. With further water uptake of the membrane, the size of the hydrophilic clusters increase and a redistribution of the sulfonic acid groups occurs [Mauritz & Moore, 2004]. The sorption behavior of Nafion® is influenced by various factors for instance temperature, equivalent weight (EW) of the membrane, and membrane pretreatment [Jalani & Datta, 2005].

In addition to the sorption behavior of the pure Nafion® membranes, the sorption behavior of the composite materials used in fuel cell manufacturing is important to characterize. This study addresses the rather less investigated area of sorption at lower ambient temperatures, present in the processing of fuel cell components. Goulet et al. showed in their studies of the sorption behavior of CCMs and MEAs that composite fuel cell components, such as the CCM, absorb

less water compared to the pure Nafion® membrane [Goulet et al., 2015]. The sorption behavior was studied by means of dynamic vapor sorption (DVS) at a temperature of 70 °C. This temperature is relevant for operating conditions of a fuel cell, but not for the manufacturing process at a production site. According to the authors, the differences in the sorption behavior can be attributed to the structure of the CCM, which consists of the Nafion® membrane and two catalyst layers [Goulet et al., 2015]. The catalyst layers are mostly composed of non-hygroscopic materials, such as carbon platinum catalyst. If the moisture uptake of the composite material is related to the ionomer mass, the authors could not find any differences in the sorption behavior of the CCM and the membrane and concluded that the ionomer can absorb the same amount of water in the composite system as long as it is free to expand in at least one direction. Along with the sorption behavior, Goulet et al. showed the effect of the water content of the polymeric membrane on the mechanical properties. In particular, at low temperatures, the absorbed water acts as a plasticizer and reduces the modulus of the membrane [Goulet et al., 2015].

Numerous studies have investigated the relation between mechanical properties and the hygroscopic behavior of Nafion® both experimentally and numerically. Tang et al. conducted tensile tests with Nafion® 112 at 16 temperature and humidity combinations in an environmental chamber [Tang et al., 2006][a]. The results have revealed a fundamental relation of Young's modulus, proportional limit stress and break stress to temperature and humidity. Furthermore, a slightly anisotropic behavior was observed between machine direction (MD) and transverse direction (TD). Kundu et al. measured the mechanical properties of both Nafion® 112 and Nafion® 117, as well as the CCM by using Nafion® 112 as substrate [Kundu et al., 2005]. Their work has indicated that the hot pressing process of catalyst layers might impact membrane morphology and consequently cause the difference between pure membranes and CCMs. Goulet et al. conducted a thoroughly comparison between pure membranes and CCMs regarding the mechanical properties change along with temperature and humidity change [Goulet et al., 2013]. An overall decrease of mechanical strength and stiffness of CCM comparing to pure membrane has been observed through tensile tests. Furthermore, they found that in the composite CCM, the catalyst layer has a reinforcing effect on the Nafion® membrane and consequently reduces the in-plane expansion during hydration, which is revealing in comparison to studies exclusively investigating the pure membrane without considering the effect of catalyst layers.

The abovementioned investigations were mostly based on the behavior of Nafion® membranes and CCMs during operation. However, this study focuses on the correlation of the day-to-day production conditions (T < 40 °C) with the mechanical properties of materials along the process chain, to generate a deep understanding of the climate conditions needed during MEA production. Based on the knowledge of the material properties alongside with a simulation model, a guidance of the micro-environment for the production will be deviated.

3   METHODOLOGY

In contrary to a large-area air conditioning, a micro-environment concept, which provides controlled local environments, offers substantial cost advantages. A micro-environment concept can be applied in not only temperature and humidity control, but also the control of cleanness, which has been widely investigated in the fields of semiconductor and flat display manufacturing [Cannella et al., 1995]. By the application of a micro-environment concept to a

MEA-fabrication, a significant reduction in the amount of air to be conditioned can be achieved. To explore the technical feasibility of this concept, a full understanding of the interactions between the materials and the conditions during production is needed.

In order to prevent this concept from possible production failures due to insufficient climate control, it is also necessary to understand the impact of humidity changes on the subassemblies. For instance, a humidity change in the early stage will cause a size inaccuracy of CCM and further disturb the location precision of the CCM. A dimensional change of CCM after lamination could induce a shear stress between CCM and subgaskets, which could exceed the permissible limits of the applied adhesive. Furthermore, a swelled MEA will also increase the difficulty of the stacking process and potentially increase the possibility of leaks. Hence, a systematic investigation on hygrothermal-induced stresses and deformations of CCMs and their effect on the other components of a MEA in different stages during the manufacturing process is needed.

To simplify the complex concept of creating a guidance for an air conditioning strategy for MEA production, the project is divided into an experimental and a simulation part. Figure 1 shows schematically the structure of the project. Input parameters of the simulative model to describe the MEA process steps are provided by sorption measurements and tensile tests of the MEA components. The numerical model of the process chain is then used to simulate the humidity-induced stresses and deformations of the MEA components. The kinetics of water sorption, which also serves as a basis for the development of a conditioning strategy, can be obtained analytically from the sorption measurements. The focus of this work is currently on the determination of the sorption behavior of the MEA components and the development of the numerical model to describe the MEA production (boxes with solid lines). Further work will deal with the implementation of the still missing experimental and analytical data (boxes with dotted lines) and the experimental validation of the concept, so that a complete guidance for the air conditioning strategy in a MEA production can be derived.
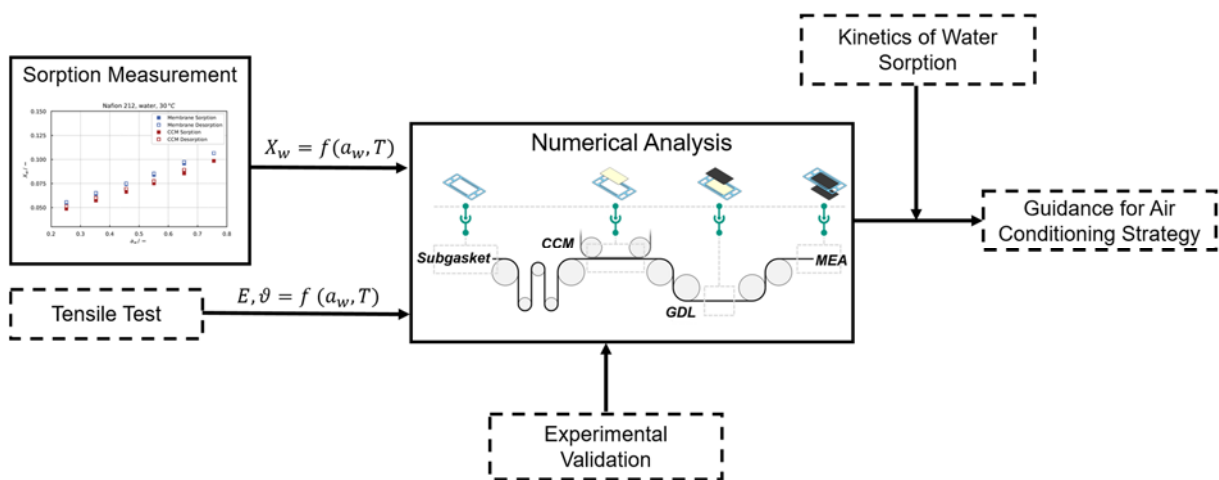

Figure 1: Methodology to develop a guidance for micro-environment concept.

4 EXPERIMENT

4.1 MATERIAL

For the characterization of the sorption behavior of the MEA components, sorption measurements are conducted on a polymer membrane and a CCM. For the polymer

membrane, Nafion® PFSA NR-212 (N212) membranes from Chemours (obtained from fuelcellstore, Texas USA) are used. In general, Nafion® membranes are characterized using the equivalent weight, the membrane thickness, and the manufacturing technique. Nafion® PFSA NR-212 has an equivalent weight of 2100 g per mole of sulfonic acid group. The measured thickness of the membrane is 50.79 ± 0.36 µm. The fabrication process of the polymer membrane determines the orientation of the polymer chains and, thus, affects the mechanical and electrical properties of the membrane. The most common manufacturing processes for Nafion® membranes are melt extrusion and dispersion casting. N212 membranes are manufactured via the dispersion casting process (manufacture's specifications [Chemours, 2021]).

For the sorption measurements of the CCM, a three-layer CCM for Hydrogen/Air Fuel Cells (obtained from fuelcellstore, Texas USA) is used. It consists of two catalyst layers on a Nafion® N212 membrane. The platinum loading of the anode and cathode is specified by the manufacturer as 0.5 mg/cm². The catalyst used is 60 wt% platinum on Vulcan XC72R (manufacturer's specifications). The three-layer CCM has a thickness of 59.25 ± 1.75 µm. For the sorption measurements, all samples are cut into circles with a diameter of 50 mm. The measured samples haven't been pretreated before performing the sorption measurements.

4.2 MAGNETIC SUSPENSION BALANCE

For the gravimetric analysis of the water content of the Nafion® membrane and the CCM under defined boundary conditions, a magnetic suspension balance was used. The experimental setup has been designed and described in detail in previous studies, such as [Schabel et al., 2003], [Mamaliga et al., 2010], [Eser et al., 2020][a] and [Eser et al., 2020][b]. In this measuring technique, the sample is placed in a temperature-controlled sorption cell made of stainless steel. The water activity in the sorption cell is adjusted by the temperature of an evaporator, from which evaporated water is fed into the sorption cell. The water activity (a_w) in the sorption cell, also relative humidity (RH) in case of water vapor, can be adjusted by the temperatures of the evaporator and the sorption cell via equation (1) [Schabel et al., 2003].

$$a_w = \frac{p_w^*\left(T_{evaporator}\right)}{p_w^*\left(T_{sorption\ cell}\right)} \qquad (1)$$

The vapor pressures (p_w^*) of water are calculated using an Antoine-equation [VDI-Gesellschaft, 2005]. The sorption cell is connected to a high-resolution microbalance by means of a magnetic coupling. This setup records the change of the sample mass over time. Using the measured mass of the absorbed water ($M_w(t)$) and the mass of the dried sample (M_{tr}), the water loading of the material (X_w) can be determined using equation (2).

$$X_w = \frac{M_w(t)}{M_{tr}} \qquad (2)$$

With this measurement setup, the activity range relevant for the processing of CCM for PEM fuel cells can be investigated with high resolution. In the activity range from 0.25 to 0.75, the sorption isotherms of the pure Nafion® N212 membrane and the three-layer CCM are studied at a constant temperature of 30 °C.

4.3 RESULTS OF THE SORPTION MEASUREMENTS

The aim of these investigations is to obtain the differences in the sorption behavior of membranes and CCM at ambient production conditions and correlate this information to the mechanical properties of the materials. For comparison, the sorption isotherms of the Nafion® N212 membrane and the three-layer Hydrogen/Air CCM are plotted in Figure 2. The graph relates the loading of the membrane and the CCM to the activity of the environment. For fuel cell component production, the interesting activity range of 0.25 to 0.75 at 30 °C for both materials is plotted.
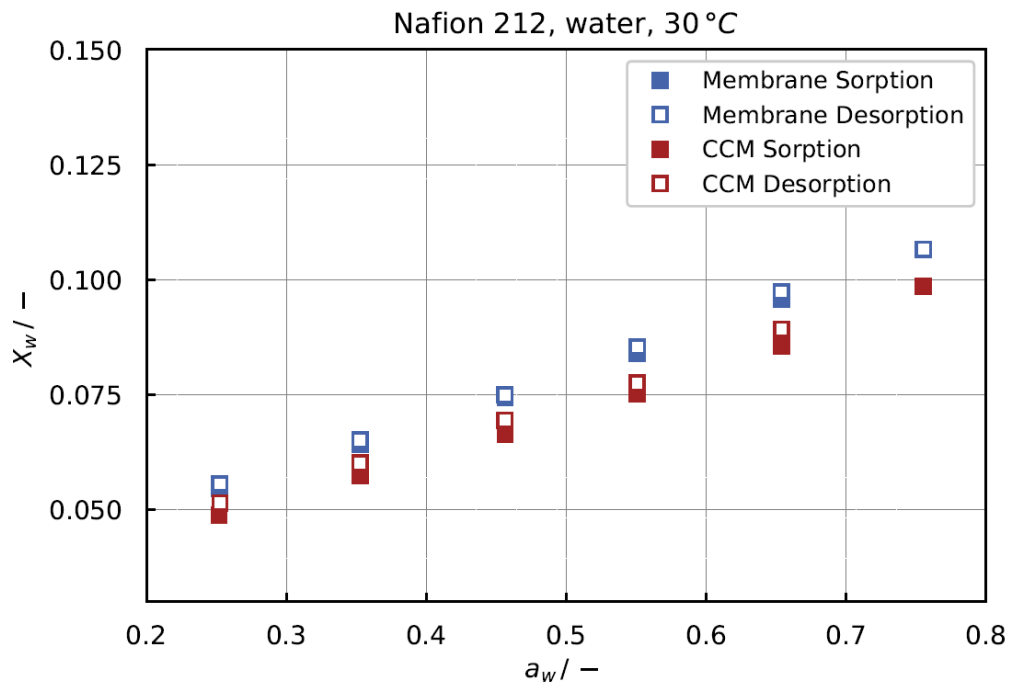

Figure 2: Sorption isotherms of Nafion® PFSA NR-212 (N212) membranes and three-layered CCM for Hydrogen/Air Fuel Cells at a temperature of 30 °C.

At a water activity of 0.25 to 0.75, the membrane has water loadings between 0.055 and 0.11. The CCM has loadings between 0.048 and 0.098 in the same activity range. When comparing the sorption behavior of the membrane with the CCM, the CCM absorbs less water at any given activity. This means that the CCM sorbs less water relative to its dry mass than the membrane. This is due to the fact that the CCM is a composite material. The composition of very hygroscopic membrane and comparatively less hygroscopic catalyst layers in the CCM is responsible for the difference in loading between CCM and membrane. The data points for the sorption and the desorption of the membrane and the CCM are regarded to be equal within the measurement uncertainty.

5 NUMERICAL MODEL AND SIMULATION

The model to simulate the manufacturing process is built up to a seven-layer MEA-construction, which consists of a both-side subgasketed CCM with full area catalyst coating as well as anode and cathode-side GDLs [Iverson et al., 2011]. The structure and cross-section of the MEA-configuration used in this work are illustrated in Figure 3.
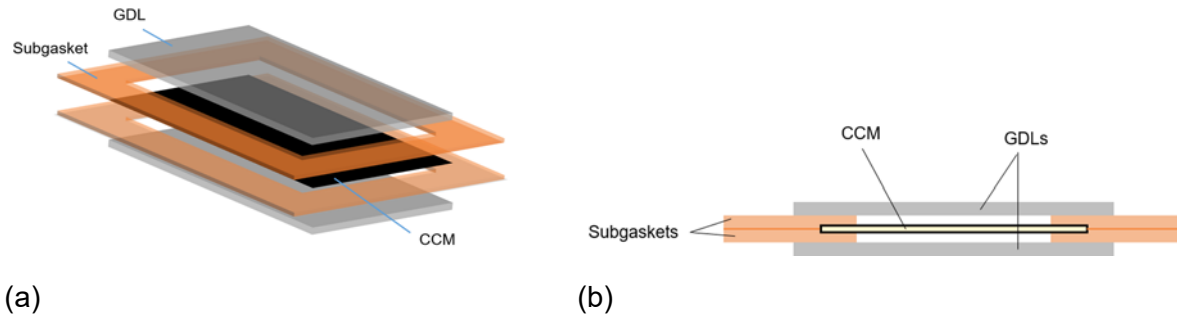
(a)   (b)

Figure 3: Schematic diagrams of the MEA-construction ((a): 3D-illustration; (b): cross-section).

5.1 GEOMETRY AND MATERIAL PROPERTIES

The simulation has been carried out using ABAQUS. In the last decade, plenty of FEM-Models have been developed and reported in the open literature (i.e. [Kusoglu et al., 2006], [Uchiyama et al., 2013]), in order to investigate the mechanical durability of the membrane under a hygrothermal cycling during fuel cell operation. Most of the models have adopted a 2D-solid model with the focus on the cross-section of a cell. However, the aim of this work is to estimate the humidity-change-induced stresses and deformations on the subassemblies in a R2R process, in which the web direction (in-plane) and the effect of web tension cannot be neglected. Since the thicknesses of all components are significant smaller than the in-plane dimensions, the 3D-shell element was selected for all the components, namely CCM, GDLs and subgaskets. The geometry parameters are shown in Table 1. Because of the complicity to acquire the accurate dimensions of PEMFC components, the values below are just assumptions according to a typical size of PEMFC in automobile area, which can be easily adjusted in the model, if needed. The subgaskets were only modeled with the window for active area, the cut-outs for the gas inlets and outlets were neglected for simplification.

Table 1: Geometry parameters of all components in the model.

	Length [mm]	Width [mm]	Thickness [mm]
CCM	200	100	0.056
Subgasket (inner)	180	90	-
Subgasket (outer)	300	150	0.125
GDL	220	120	0.280

According to the current state of art, there are generally two approaches to model the CCM [Khorasany et al., 2014]. One is to regard them as three separate layers with tie constraints, which requires an approximation of the material properties of catalyst layers. The other one is to treat the CCM as one single component, whose mechanical properties can be extracted directly from tensile tests or similar. In this work, the second approach was adopted. As aforementioned, the hygrothermal mechanical properties of Nafion® membrane have been extensively studied. Yet, the experimental data for CCM is relatively rare. In the work of Goulet et al. experimental tests were conducted on CCMs for 50 % and 70 % RH at 23 °C and 70 °C [Goulet et al., 2013]. The literature values have served as inputs for the present MEA model and the values between the given temperature and humidity field were interpolated by

ABAQUS. The mechanical properties were implemented into the simulation model through the ABAQUS built-in material model. The total strain can be divided into mechanical, thermal expansion and swelling strains as shown in equations (3) to (5) [Tang et al., 2006][b].

$$\varepsilon = \varepsilon^M + \varepsilon^T + \varepsilon^{RH} \qquad (3)$$

$$\varepsilon^T = \alpha\,\Delta T \qquad (4)$$

$$\varepsilon^{RH} = \beta\,\Delta RH \qquad (5)$$

α and β are the thermal expansion and swelling coefficient. Correspondingly, ΔT and ΔRH represent the temperature and relative humidity change. Hence, a user-defined subroutine UEXPAN and a predefined humidity field are implemented in the model.

Additional to the CCM the GDL is also a key factor to build the model. The material properties of GDLs in this current model were adopted from the works of Lu et al. and Kleemann et al., who have reported an anisotropic elastic behavior of commercial GDL products from different manufacturers ([Lu et al., 2011], [Kleemann et al., 2009]). Their experimental investigations indicate significantly lower elastic properties in the thickness direction in comparison to the in-plane elastic properties. Furthermore, no dependencies of Young's modulus on temperature and humidity have been detected. The same parameters were adopted into this model for GDLs and listed in Table 2. The polyimide film Kapton™ is often used as subgasket to increase the strength of the membrane. In the current model, the material properties of the 125 µm Kapton™-film were taken [DuPont, 2019]. All material properties used in this FEM simulation are listed in Table 2.

Table 2: Material properties from literature values used in FEM simulation.

Material	E [MPa]	ϑ	$\alpha\ [K^{-1}]$	$\beta\ [\%^{-1}]$
CCM (T=23 °C)	50 % *RH*: 172 70 % *RH*: 95	0.3	7.21×10^{-4}	4.84×10^{-4}
GDL	$E_x = E_y = 1500$; $E_z = 9$	$\vartheta_{xz} = \vartheta_{xy} = \vartheta_{zy} = 0$	Neglected	Neglected
Subgasket	2760	0.34	Neglected	Neglected

5.2 BOUNDARY CONDITIONS AND SIMULATION PROCEDURE

In order to simulate the fabrication conditions, different boundary conditions were taken into account. For a R2R process, the effect of the web tension is non-negligible, which was treated in this model as a uniformly distributed force on the subgasket edges. In the work of Park et al., a web tension of 0.065 N/mm was applied to a 200 mm wide Nafion® membrane web with the support of a 100-µm-thick polyester film [Park et al., 2020]. Chen et al. have reported a R2R equipment to fabricate a five-layer MEA, in which the membrane with protective films has served as the main web. A web tension around about 0.037 N/mm was measured by tension rollers [Chen et al., 2016]. Hence, in this model the web tension was set up to 0.05 N/mm on the right edges of the subgaskets, while the left edges were assigned with encastre constraints. A surface-based cohesive contact was employed to define the adhesive interaction between subgaskets and CCM / GDLs, since the thickness of the interface is only couple microns and

therefore negligible. On top of that, modelling the adhesive layer by using surface-based cohesive behavior also offers the possibility to define surfaces that are not initially bonded but will come to contact in the subsequent steps, which is advantageous to simulate the discrete steps in a MEA production line. Unlike the most of the durability studies of PEMFC, which emphasize the hygrothermal cycling during the fuel cell operation for automotive applications (up to 80 °C), the temperature change in a factory could be approximately estimated between 20 and 30 °C. Randová et al. found in their studies on the sorption behavior of Nafion® membranes that in a temperature range of 15 to 38 °C, the temperature has no effect on the water uptake of the polymer membrane [Randová et al., 2015]. Therefore, the temperature was set up to room temperature (23 °C) and remains constant during the whole simulation. A humidity field was pre-defined in each step and changed through interface scripting.

To simulate an assembly procedure during a R2R-Process, four steps were created in the FEM simulation:

Step-1: The web tension was applied in the form of a shell edge load on the subgaskets. Initial temperature and humidity field were set up to 23 °C and 50 % RH (ideal conditions). The temperature was held constant throughout the rest of the simulation.

Step-2: The CCM was disposed between two subgaskets with adhesive components. The humidity was changed linearly from the initial conditions to the next humidity level (RH1).

Step-3: One GDL was glued on the bottom of the subgasketed CCM. The humidity level was again modified (RH2).

Step-4: The other GDL was attached to the other side of subgasketed CCM to form a seven-layer MEA. The humidity level was set up to the next potential value (RH3).

5.3 SIMULATION RESULTS

A statistical design of experiments (DoE) approach was employed to investigate the effect of humidity change in different assembly steps (RH1, RH2 and RH3) on subassemblies and consequently to define customized humidity requirements and economic condition strategy. Due to the lack of experimental data and literature values, the humidity range for DoE was firstly chosen between 50 % and 70 %.

The first investigation has demonstrated a relatively extreme scenario, in which the humidity level first rose up to 70 % from the initial state (50 %), after the CCM was encapsulated between two subgaskets (step-2). In the following production processes, the humidity first decreased to 60 % in step-3 and then to 50 % in step-4. The von Mises stress contours on the surface of the CCM from step-2 to step-4 are shown in Figure 4(a)-(c). The stress contour in step-1 is not shown here, since the CCM experiences no stress in this step. Figure 4(d) shows the same stresses along a path in the middle of the CCM in machine direction.
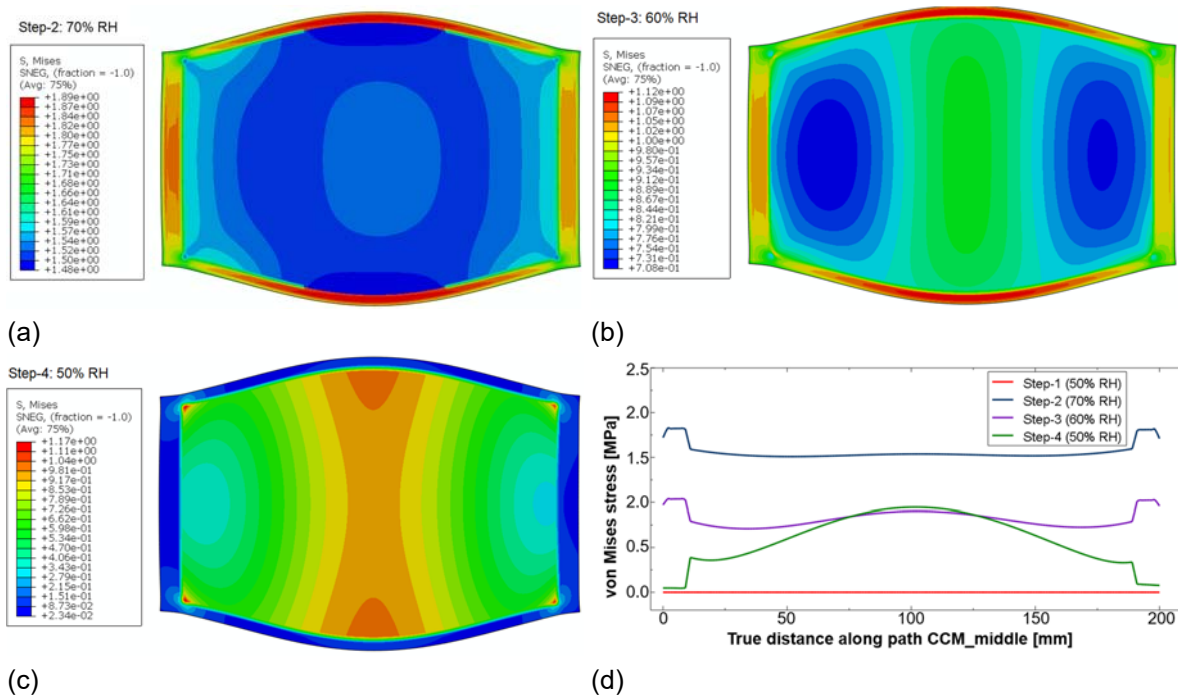
Figure 4: Von Mises stress states of the CCM under humidity changes: stress contours (a) 70 % RH in step-2, (b) 60 % RH in step-3, (c) 50 % RH in step-4 and (d) stress distribution along the middle path of CCM in machine direction.

It can be observed in Figure 4(a) that the humidity change from 50 % to 70 % has initiate water uptake and swelling effect of CCM, whereas the edge-constraints by subgaskets have impeded the swelling. Thus, the stress amplitude in the contact area with the subgaskets is higher than that of the central region. In the following dehydration process (Figure 4(b) and (c)) the CCM shows a tendency to shrink back to the original status. However, the subgaskets, and the attached GDLs with greater thickness and much higher stiffness hinder the contraction of the CCM. Hence, there is a higher concentrated stress in the middle area in the last step, which can be seen in Figure 4(d) with the green line. The purple line, which stands for the stress distributions in step-3, also shows a similar hump-shaped tendency in the middle area, but not as significant as in the last step. Presumably, the attachment of the second GDL further stiffens the subassembly and consequently prevents the CCM from shrinkage even more.

To further investigate and define the most critical step for a potential humidity change, three different simulations were conducted, in which the humidity level was changed to 70 % in step-2, step-3 and step-4, respectively, and the other steps remained 50 %. A plot of the maximum in-plane strain of the CCM in each step for all three simulation procedures are illustrated in Figure 5(a).
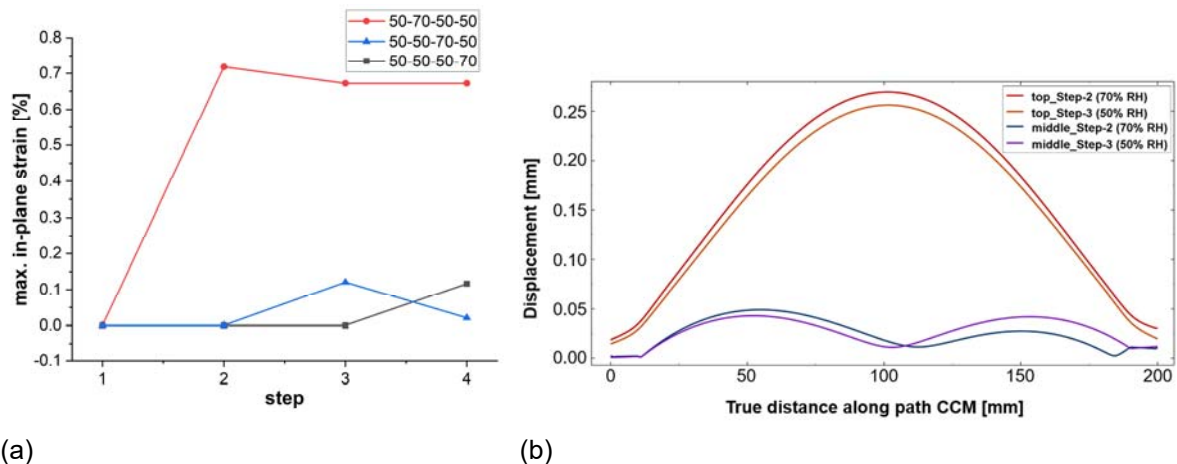
Figure 5: (a) The maximum in-plane strain of the CCM in each step for all three simulation procedures (50-70-50-50, 50-50-70-50 and 50-50-50-70), (b) The displacement along top edge and middle line of CCM for 50-70-50-50.

It can be seen that an increase of humidity induces notably more in-plane strain (0.7 %) in step-2 than in step-3 and 4, which is also not able to return back to near zero, even though the humidity level was reset to 50 % afterwards. To better understand the mechanism for this phenomenon, the distribution of displacement along the top edge and middle line of the CCM in step-2 and 3 for simulation 50-70-50-50 is plotted in Figure 5(b). The displacement distribution differs substantially between the top edge and the middle area of the CCM. The maximum displacement is in the transverse direction on both edges. This confirms the assumption that the CCM is easier to swell without the attachment of GDLs on the subgaskets, and especially in the transverse direction without mechanical strains. Which means, a humidity increase could be more crucial in the CCM bonding process than after the attachment of the first GDL.

6   SUMMARY AND OUTLOOK

A comparison between the sorption behavior of the pure membrane and the CCM has been conducted experimentally. It was shown, that the CCM sorbs less water relative to its dry mass compared to the pure Nafion® membrane. Based on the sorption results, correlations between the mechanical properties and the loading of the components at specific ambient conditions will be further investigated. Furthermore, the kinetics of water uptake will be used to model the time-dependent water sorption behavior of the membrane and the CCM in order to provide guidance for the design of the air conditioning for the process chain of the MEA production.

A general approach to build a MEA model to simulate production processes with local climate control has been provided. The corresponding numerical analysis was carried out in ABAQUS under simultaneously combined hygro-mechanical conditions. An insight into the magnitude of humidity-change-induced stresses and deformations could also be gained from the simulation results. It can be derived from the simulation results, that a precise humidity control in the area before the attachment of GDLs could still be essential. The process after the attachment of the

first GDL could be less strict, as long as the ambient humidity is set back to 50 % at the end of the process chain.

ACKNOWLEDGEMENTS

REFERENCES

[Cannella et al., 1995]   Cannella, V., Vijan, M. & Gregg, A., (1995). The use of minienvironments in AMLCD and other FPD manufacturing. *Proceedings of Second International Workshop on Active Matrix Liquid Crystal Displays*, pp. 37-41. doi: 10.1109/AMLCD.1995.541091

[Chemours, 2021]   Chemours, (2021). *nafion.de.* [Online] Available at: https://www.nafion.de/products/sulfonic-membranes [Zugriff am 08 10 2021].

[Chen et al., 2016]   Chen, J., Liu, H., Huang, Y. & Yin, Z., (2016). High-rate roll-to-roll stack and lamination of multilayer structured membrane electrode assembly. *Journal of Manufacturing Processes*, pp. 175-182. http://dx.doi.org/10.1016/j.jmapro.2016.06.022

[DuPont, 2019]   DuPont, (2019). *DEC-Kapton-HN-datasheet.* [Online] Available at: https://www.dupont.com/content/dam/dupont/amer/us/en/products/ei-transformation/documents/DEC-Kapton-HN-datasheet.pdf [Zugriff am 18 09 2021].

[Eser et al., 2020][a]   Eser, J. C. et al., (2020). Diffusion kinetics of water in graphite anodes for Li-ion batteries. *Drying Technology*, pp. 1-16. 10.1080/07373937.2020.1852568

[Eser et al., 2020][b]   Eser, J. C. et al., (2020). Moisture Adsorption Behavior in Anodes for Li-Ion Batteries. *Energy Technol. 8*, p. 1801162. https://doi.org/10.1002/ente.201801162

[Fey et al., 2010]   Fey, M. M. et al., (2010). *Catalyst Coated Diffusion Media.* US, Patentnr. US 7651581B2.

[Goulet et al., 2015]   Goulet, M.-A., Arbour, S., Lauritzen, M. & Kjeang, E., (2015). Water sorption and expansion of an ionomer membrane constrained by fuel cell electrodes. *Journal of Power Sources*, pp. 94-100. http://dx.doi.org/10.1016/j.jpowsour.2014.10.040

[Goulet et al., 2013]   Goulet, M.-A.et al., (2013). Mechanical properties of catalyst coated membranes for fuel cells. *Journal of Power Sources*, pp. 38-47. http://dx.doi.org/10.1016/j.jpowsour.2013.01.128

[Iverson et al., 2011]   Iverson, E. J., Pierpont, D. M., Yandrasits, M. A. & Hamrock, S. J., (2011). *Fuel cell subassemblies incorporating subgasketed thrifted membranes.* US, Patent No. US 2011/0151350 A1.

[Jalani & Datta, 2005]   Jalani, N. H. & Datta, R., (2005). The effect of equivalent weight, temperature, cationic forms, sorbates, and nanoinorganic additives on the sorption behavior of Nafion®. *Journal of Membrane Science*, pp. 167-175. https://doi.org/10.1016/j.memsci.2005.04.047

[James et al., 2008]   James, R. L., Valentine, S. D. & Leistra, J., (2008). *Manufacture or Membrane Electrode Assembly with Edge Protection for PEM Fuel Cells.* US, Patentnr. US 2008/01105354 A1.

[Khorasany et al., 2014]   Khorasany, R. M. et al., (2014). On the constitutive relations for catalyst coated membrane applied to in-situ fuel cell modeling. *Journal of Power Sources*, pp. 176-188. http://dx.doi.org/10.1016/j.jpowsour.2013.11.087

[Kim et al., 2015]   Kim, D. K., Choi, E. J., Song, H. H. & Kim, M. S., (2015). Experimental and numerical study on the water transport behavior through Nafion® 117 for polymer electrolyte membrane fuel cell. *Journal of Membrane Science*, pp. 194-208. http://dx.doi.org/10.1016/j.memsci.2015.09.053

[Kleemann et al., 2009]   Kleemann, J., Finsterwalder, F. & Tillmetz, W., (2009). Characterisation of mechanical behaviour and coupled electrical properties of polymer electrolyte membrane fuel cell gas diffusion layers. *Journal of Power Sources*, p. 92–102. 10.1016/j.jpowsour.2008.09.026

[Kundu et al., 2005]   Kundu, S., Simon, L. C., Fowler, M. & Grot, S., (2005). Mechanical properties of Nafion electrolyte membranes under hydrated conditions. *The International Journal for the Science and Technology of Polymers*, pp. 11707-11715. doi:10.1016/j.polymer.2005.09.059

[Kusoglu et al., 2006]   Kusoglu, A. et al., (2006). Mechanical response of fuel cell membranes subjected to a hygro-thermal cycle. *Journal of Power Sources*, p. 987–996. doi:10.1016/j.jpowsour.2006.05.020

[Lu et al., 2011]   Lu, Z. et al., (2011). Effect of gas diffusion layer modulus and land–groove geometry on membrane stresses in proton exchange membrane fuel cells. *Journal of Power Sources*, 15 May, p. 4646–4654. https://doi.org/10.1016/j.jpowsour.2011.01.028

[Mamaliga et al., 2010]   Mamaliga, I., Schabel, W. & Petrescu, S., (2010). Characterization of Water Vapour Diffusion into Spherical Silica Gel Particles. *Revista de Chimie 61(12)*, pp. 1231-1234.

[Mauritz & Moore, 2004]   Mauritz, K. A. & Moore, R. B., (2004). State of Understanding of Nafion. *Chemical reviews*, p. 4535–4585. 10.1021/cr0207123

[Park et al., 2020]   Park, J. et al., (2020). Roll-to-roll production of catalyst coated membranes for low-temperature electrolyzers. *Journal of Power Sources*. https://doi.org/10.1016/j.jpowsour.2020.228819

[Randová et al., 2015]   Randová, A. et al., (2015). Sorption of enantiomers and alcohols into Nafion® and the role of air humidity in the experimental data evaluation. *Separation and Purification Technology*, p. 232–239. 10.1016/j.seppur.2015.02.045

[Schabel et al., 2003]   Schabel, W., Mamaliga, I. & Kind, M., (2003). Messungen von Sorptionsisothermen und Diffusionskoeffizienten in Polymerlösungen. *Chemie-Ingenieur-Technik*, pp. 36-41.

[Tang et al., 2006][a]   Tang, Y. et al., (2006). An experimental investigation of humidity and temperature effects on the mechanical properties of perfluorosulfonic acid membrane. *Materials Science and Engineering*, p. 297–304. doi:10.1016/j.msea.2006.03.055

[Tang et al., 2006][b]   Tang, Y., Santare, M. H. & Karlsson, A. M., (2006). Stresses in Proton Exchange Membranes Due to Hygro-Thermal Loading. *Journal of Fuel Cell Science and Technology*, pp. 119-124. 10.1115/1.2173666

[Töpler & Lehmann, 2014] Töpler, J. & Lehmann, J., (2014). *Wasserstoff und Brennstoffzelle.* Heidelberg: Springer-Verlag Berlin. 10.1007/978-3-642-37415-9

[Uchiyama et al., 2013]   Uchiyama, T., Kumei, H. & Yoshida, T., (2013). Catalyst layer cracks by buckling deformation of membrane electrode assemblies under humidity cycles and mitigation methods. *Journal of Power Sources*, pp. 403-412. http://dx.doi.org/10.1016/j.jpowsour.2013.04.026

[Valentine et al., 2009]   Valentine, S., James, R. L., Healy, J. P. & Lakshmanan, B., (2009). *MANUFACTURE OF UNITIZED ELECTRODE ASSEMBLY FOR PEMFUEL CELLS.* USA, Patentnr. US 7569082 B2.

[VDI-Gesellschaft, 2005] VDI-Gesellschaft, (2005). *VDI-Wärmeatlas.* 5. Hrsg. Wiesbaden: Springer Berlin Heidelberg.